

Response of Railway Steel Bridges to Rail and Wheel Defects

Hanan H. Eltobgy, Ahmed Abdel Moamen Khalil, Emad E. Darwish, Mohamed Saber

Abstract— This paper aims to investigate the structural behaviour of railway steel bridges due to track defects, such as abnormal rail or wheel surfaces, rail corrugation, rail wear or breakage, as well as wheel flats. The dynamic models were established using the application of the finite element software ABAQUS to simulate the structure as a train-track-bridge (TTB) interaction model. Benha's railway steel-truss-bridge was used in this study. The part simulated of the bridge's superstructure consisted of 2 spans, in total lengths of 124.8 meters. The train runs through open deck floor (i.e., non-ballasted track). The track is fixed directly to the bridge stringers. The FEMs in the TTB category were established to study the effect of rail defects on the bridge's elements response (acceleration and strains) and to predict the dynamic amplification factors. Results obtained from the TTB models, related to the simulation of track defects were compared against those mentioned in both Euro and UIC codes. The response for all defects inherent with the dynamic amplification increased by 10% and 20% for the cross girders and stringers, respectively. Defected Track had a significant effect on the bridge acceleration, displacement, and strains. FEM results exceeded the allowable limit proposed by the international codes.

INDEX TERMS— STEEL BRIDGES, TRAIN-TRACK-BRIDGE, DYNAMIC AMPLIFICATION FACTOR, RAIL CORRUGATION, WEAR, WHEEL FLAT.

1 INTRODUCTION

Railway bridges are considered critical elements of any railway network. The railway track on the bridge deck was subdivided into three categories: Open Bridge Deck, Ballasted Deck Bridge, and Direct Fixation Deck [1]. Tracks have a significant role in the railway system as their defects are the most frequent cause of train derailments; in addition to their direct impact on the bridge structural behaviour due to the train-track-bridge (TTB) interaction phenomenon. TTB interaction phenomenon has very prominent role on the bridge's response. The dynamic impact on the structural elements of the bridge resulted from the train speed, produces abnormal behaviour due to rail defects, thus, directly influences the working status and the bridge service life. On the other hand, the unexpected behaviour of bridge structure due to track defects affects in turn the running safety and stability of trains movement over bridges. Therefore, the structural behaviour of the TTB system associated with track defects represents a fundamental problem that requisite careful consideration in the design of bridges. Thus, it has become a mandatory to carry out extensive studies on the dynamic interaction along with the train and bridge systems. In view of that, it was necessary to take into consideration the influence of track de-

fects on the bridge's response in simulating the railway track structures inherent with the TTB interaction phenomena. The track's random irregularity has remarkable effect on the TTB dynamic interaction, especially in the high-speed operation. The existing track random irregularity should be considered in the simulation of the dynamic TTB interactions [2].

The track irregularities can be analysed in the railway bridge design through the dynamic amplification factor equations described in international union code of railway UIC 776-1R [3] and European code EN 1991-2 [4].

The track irregularities included in the dynamic amplification factor were assumed as a vertical dip 2mm, and 6mm existing in the track over lengths of 1.0m, and 3.0m, respectively, under unsprung mass of 2t per axle [5]. The dynamic amplification is usually aggravated with low quality railway tracks and the effect of track irregularity of various wavelengths triggered obvious changes in the bridge fundamental frequency occurred during train passages [6]-[8]. Furthermore, the shorter wavelengths represented important factors for safety analyses (wheel-rail forces) and structural assessment, while longer wavelengths related more to the vehicle ride quality [9]. The dynamic amplification at critical speed was found to be approximately 2.5 times larger compared with those values recommended by codes [10]. Random vertical track irregularities contributed to high frequency oscillations with large amplitudes in vertical accelerations of the composite (steel - concrete) bridge Marian [11]. Local rail and wheel defects produced large amplitude excitations compared to smooth track. Type of rail defect has a major impact on vibration levels [12]. Wheel/rail irregularities such as spalling, rail corrugation, wheel out of roundness, and flat spots could significantly increase the dynamic effect, particularly at high-speed [13, 14]. The track-short defects such as loose fishplate bolts as well as

Hanan H. Eltobgy, Associate Professor Steel Structures and Bridges, Civil Eng. Department, Faculty of Engineering, Shoubra, Benha University, Egypt. E-mail: hanan.eltobgy@feng.bu.edu.eg

Ahmed Abdel Moamen Khalil, Associate Professor, Railway Engineering Civil Eng. Department, Faculty of Engineering, Shoubra, Benha University, Egypt. E-mail: ahmed.khalil@feng.bu.edu.eg

Emad Darwish, Lecturer, Civil Eng. Department, Faculty of Engineering, Shoubra, Benha University, Egypt. E-mail: emad.darwish@feng.bu.edu.eg

Mohamed Saber, Department of Structural Engineering, Egyptian Company for Cairo Metro (ECM), Cairo, Egypt. E-mail:

eng.mohamedsaber01@gmail.com

the contact between fishplates and the rail head produced large contact force variation [15]. Track spectrums as described by the power spectral density (PSD) are commonly used to generate the random track irregularities [16]. [17] studied structural behaviour of railway steel bridges due to track defects. [18] investigated the behaviour of steel railway bridges under the effect defected rail welds.

The current study meant to investigate the structural behaviour of railway steel bridges due to the most critical track defects liable to produce dynamic effect resulting from the rolling contact between wheel and rail. These defects as identified by [5], include rail corrugation, excessive rail wear, rail breakage, worn wheel (flats or spots), and defects of welded or jointed rail. The study used the finite element program ABAQUS [19] taking into consideration the TTB interaction phenomenon. Regarding the simulation of the interaction between train and bogies suspension system, the train car body and their bogies were modelled as rigid beams [6]. Bogies' masses and train car body were replicated as mass elements, including the translational and rotational inertial properties of each, focussing in the middle point of the rigid elements. The suspension systems were modelled as spring-dashpot assembly.

2 DESCRIPTION OF BRIDGE

Bridge: Benha Bridge is one of the steel rail-way bridges that has been built in Egypt since 1965, located on Damietta branch of the Nile River at 46.290 km on Cairo-Alexandria railway track as defined by the Egyptian National Railway Authority, ENR. The bridge has a total length of 320m divided into five bays. Four bays consist of two continuous spans and a simply supported middle bay swing span. This work focuses on the continuous spans at the end of the bridge (62.4 m). The

structural system of Benha railway bridge is drawn in figs.1- 3. The substructure of the bridge consists of seven reinforced concrete supports (Five piers inside the Nile and two abutments on both sides). The bridge superstructure is made of warren trusses assembled by rivets with constant depth of 8.0 m, and with upper and lower bracing system. The distance between main trusses is 9.15 m. The bridge also has a transversal cross-sectional portal frames arranged every 6.3m. All bridge elements were made of built-up sections connected with lacing bars and batten plates of steel ST-52, with yield stresses 3.6 t/cm², ultimate stress 5.2t/cm², modulus of elasticity 2100 t/cm², mass density 7.85 t/m³, and Poisson's ratio 0.3. However, the main truss elements, stringers and cross girders are simulated in the FEM with equivalent sections as described in Table 1.

Track: double track lines are passing through Benha bridge, supported on non-blasted, open deck floor. The rails are seated on timber sleepers and fixed directly to the bridge stringers. The track is divided into three disconnected parts of tracks along the bridge (rail of each one is connected by the continuous welded rail (CWR) technique). Two expansion joints are located on bridge ends in addition to, two track joints located on both ends of the simply supported middle swing bay.

Train: The train is Henschel locomotive type in total weight of 128.4 ton loaded on six-wheel sets. Henschel locomotive has two identical bogies with three wheelsets each length of the locomotive is about 22 m as shown in fig. 4. The maximum permissible speed of the train is 120 km/h during bridge's crossing.



Fig. 1. Benha railway steel bridge (a) Elevation, (b) Track and (c) Side view

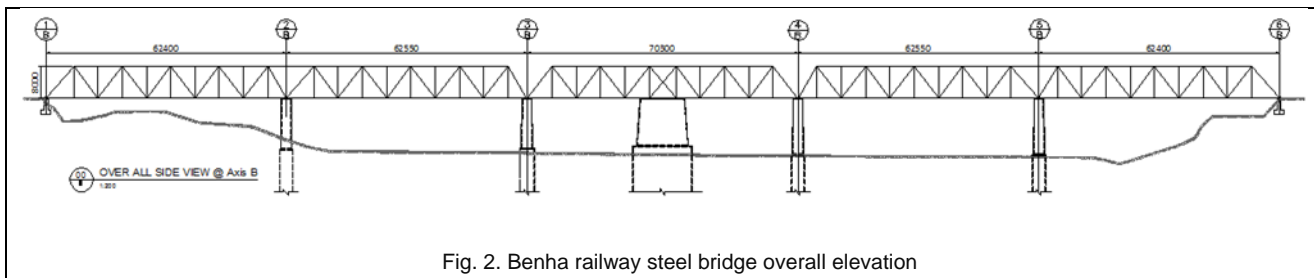


Fig. 2. Benha railway steel bridge overall elevation

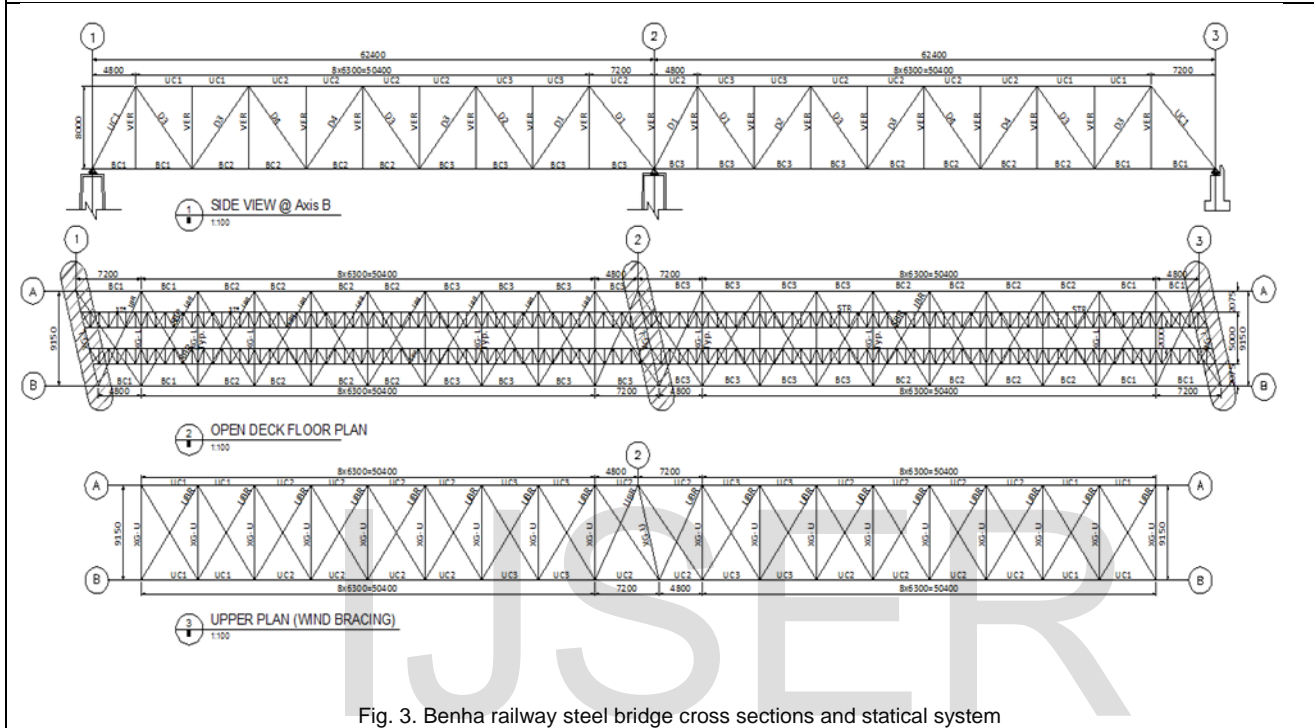
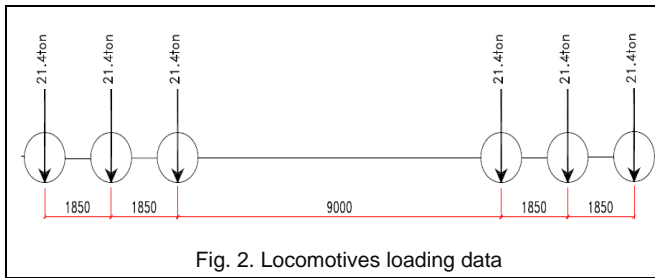


Fig. 3. Benha railway steel bridge cross sections and statical system

TABLE 1
 STEEL SECTION PROFILES BASED ON BRIDGE DESIGN DRAWINGS

| Section | Profile | B _{ft} | B _{fb} | T _{ft} | T _{fb} | dw | tw | PROFILE |
|---------|-----------|-----------------|-----------------|-----------------|-----------------|------|----|---------------------------------|
| XG-L | I-Section | 350 | 350 | 40 | 40 | 1100 | 20 | <p>I-SECTION</p> |
| XG-U | I-Section | 280 | 280 | 25 | 25 | 550 | 12 | |
| STR | I-Section | 250 | 250 | 25 | 25 | 850 | 10 | |
| BC1 | 2C-[RHS] | 550 | 550 | 6 | 6 | 500 | 14 | <p>S/RHS Hollow Section</p> |
| BC2 | 2C-[RHS] | 550 | 550 | 6 | 6 | 500 | 36 | |
| BC3 | 2C-[RHS] | 550 | 550 | 6 | 6 | 500 | 30 | |
| UC1 | 2C-[RHS] | 550 | 550 | 10 | 10 | 500 | 26 | <p>L - Section</p> |
| UC2 | 2C-[RHS] | 550 | 550 | 15 | 15 | 500 | 15 | |
| UC3 | 2C-[RHS] | 550 | 550 | 10 | 10 | 500 | 16 | |
| VER | I-Section | 300 | 300 | 25 | 25 | 500 | 11 | |
| D1 | I-Section | 400 | 400 | 45 | 45 | 500 | 20 | |
| D2 | 2C-[RHS] | 450 | 450 | 13 | 13 | 400 | 28 | |
| D3 | 2C-[RHS] | 450 | 450 | 10 | 10 | 400 | 18 | |
| D4 | 2C-[RHS] | 450 | 450 | 6 | 6 | 400 | 12 | |
| UBR | 2C-[RHS] | 160 | 160 | 8 | 8 | 400 | 4 | |
| LBR | 2L-[TS] | 125 | -- | 12 | -- | 140 | 25 | |
| SBR | L-Section | 100 | -- | 10 | -- | 100 | 10 | |



3. FEM AND NUMERICAL ANALYSIS

3D FEM was performed to investigate the performance of the bridge structural elements under the effect of track defects using ABAQUS 2017 [19]. The FEM were developed to study the influence of track defects on the bridge response, acceleration, strains of bridge stringers and cross girders, and predict the dynamic amplification factors associated with each type of simulated defect. TTB model results related to the simulation of the proposed track defects were compared with those calculated or recommended by international codes [4], [5].

3.1 FEM for Steel Bridge and Track Structures

The bridge is restrained by hinged supports in the middle of the continuous spans, and roller supports at both ends. Joint connections of main truss elements were assumed to be rigid while connections between cross girder and bracing were hinge. Connection between rails (solid elements) and sleepers were assumed to be pin connection.

Rails are made of steel grade R260 according to EN13674 specs, with tensile strength varies from 8.80-11.75 t/cm², and modulus of elasticity 2100 t/cm², mass density 7.85 t/m³, and Poisson's ratio 0.3. Rails dimensions are coinciding with [5], simulated as a solid extrusion element as shown in fig5.

The wheels are made of steel with modulus of elasticity 2100 t/cm², mass density 7.85 t/m³, and Poisson's ratio 0.3, assumed to be 800mm in diameter and simulated as a solid revolution element. Simulation of wheel meshing size is (4608) linear hexahedral elements (C3D8R) is shown in fig6.

The sleepers are made of wood with modulus of elasticity 8.412 t/cm², mass density 1.096 t/m³, and Poisson's ratio 0.25. All sleepers were simulated as beam element with dimensions 250x150x2600mm are shown in fig7.

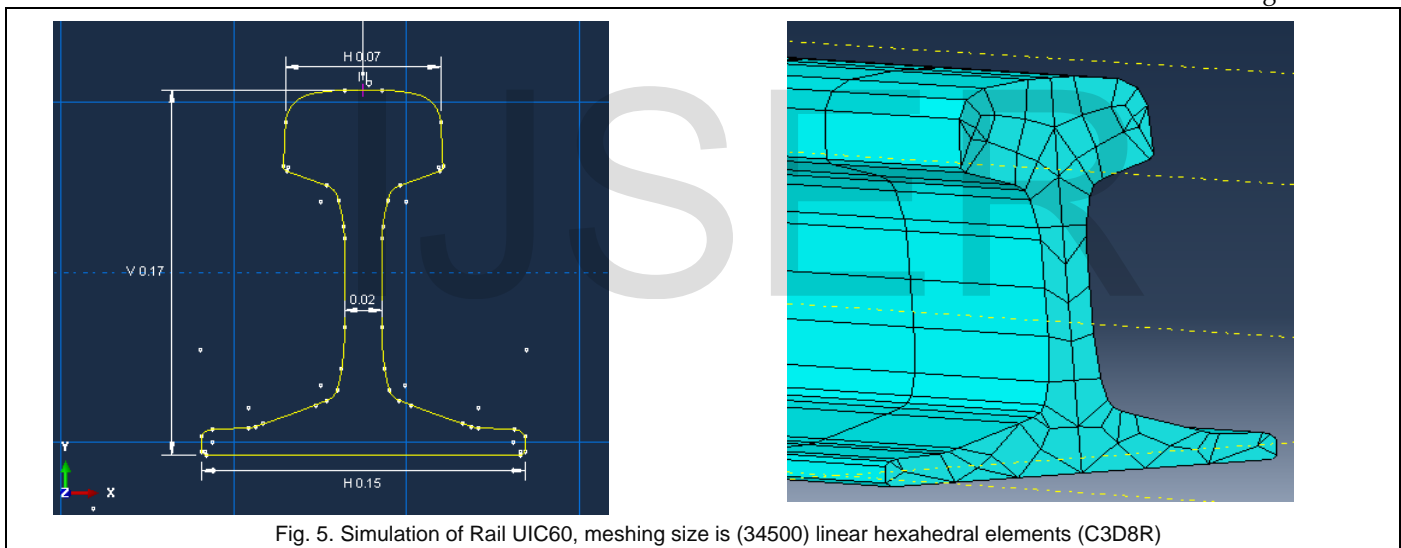


Fig. 5. Simulation of Rail UIC60, meshing size is (34500) linear hexahedral elements (C3D8R)

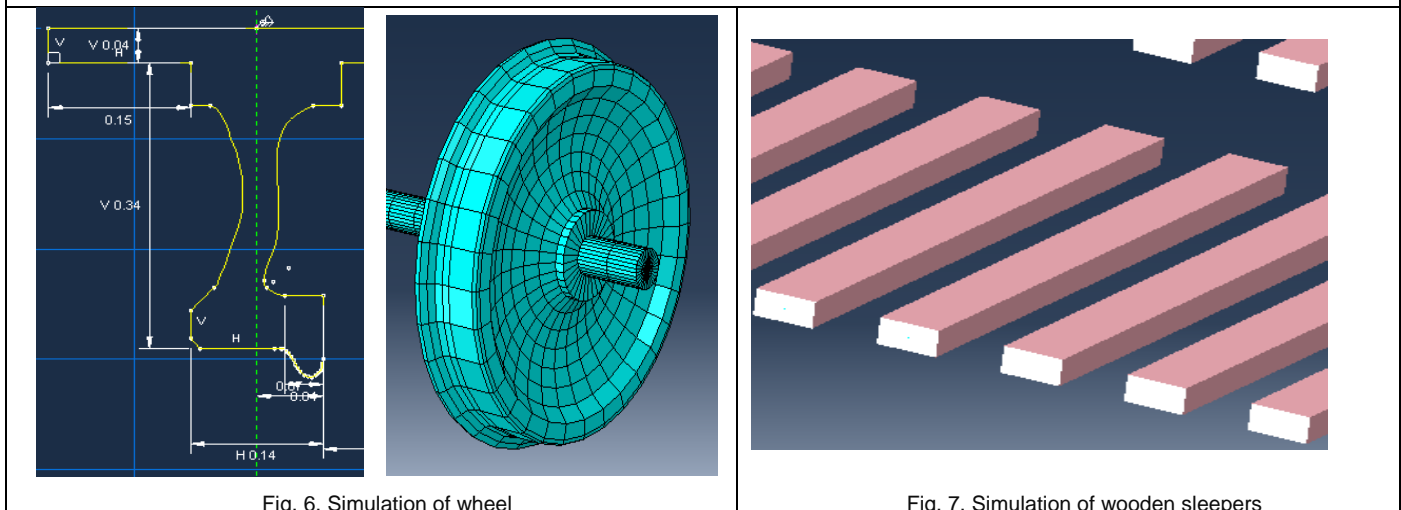


Fig. 6. Simulation of wheel

Fig. 7. Simulation of wooden sleepers

3.2 TTB model

Figs. 8, 9 present the schematic diagram of TTB system used in the FEM. Nonlinear 3D spring-damper elements were used to represent the suspension model between wheel and Bogie Connection. The Henschel bogies were simulated with spring stiffness 66500N.m/m and dashpot coefficient 53000 N.m/m.

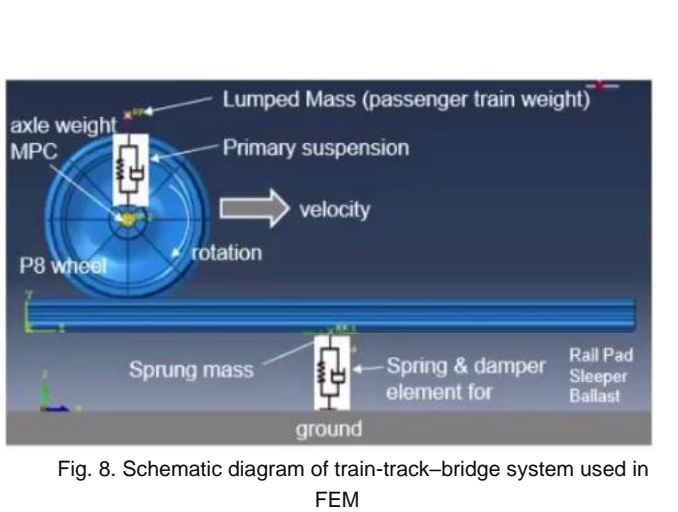


Fig. 8. Schematic diagram of train-track-bridge system used in FEM

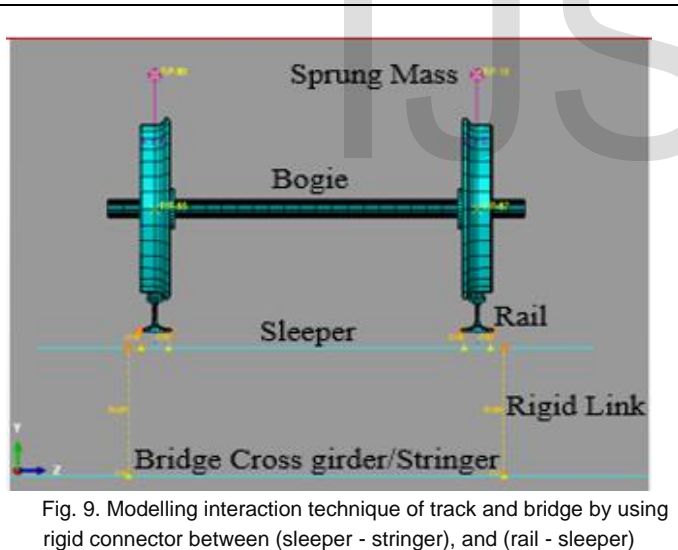


Fig. 9. Modelling interaction technique of track and bridge by using rigid connector between (sleeper - stringer), and (rail - sleeper)

ABAQUS wire feature was used to represent the relation between rail and sleeper or between the sleeper and stringers beam connector section. In this study, the interaction between rail-sleeper and sleeper-stringer were taken into consideration by the concept of rigid link. The wheel and rail interacted using surface-to-surface hard contact with friction coefficient of 0.30 as shown in fig.10. The track was assumed to start 30m before the beginning of the bridge, that was assumed to be supported directly on a subgrade soil simulated as a fixed support.

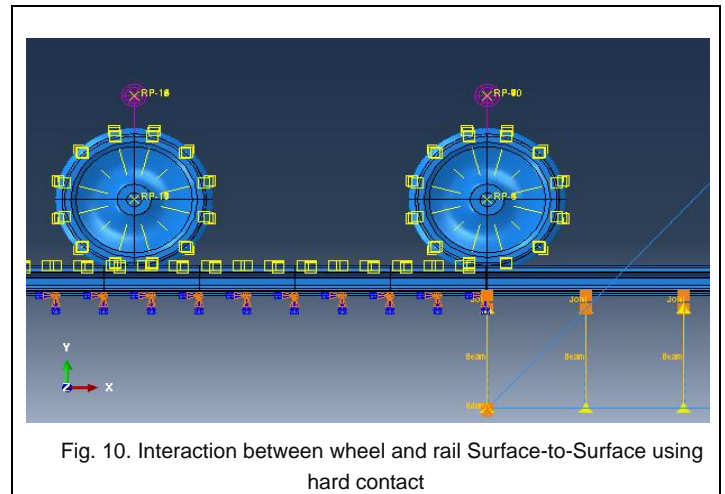
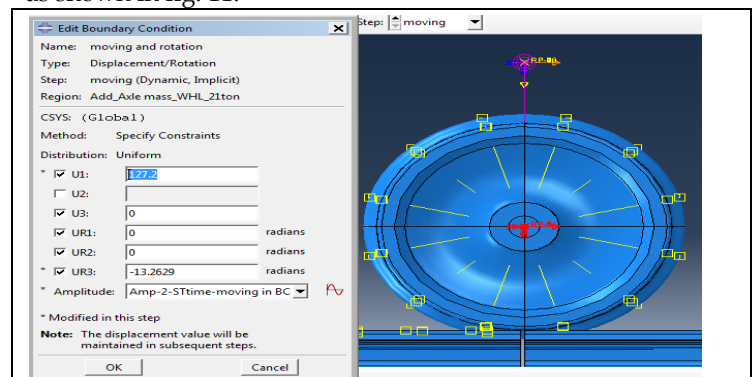


Fig. 10. Interaction between wheel and rail Surface-to-Surface using hard contact

3.3 Boundary Conditions

The two vertical warren trusses of the main girders are supported as a hinged support at the middle of the two continuous spans, while assigned as a roller supports at spans' ends. The 4 rails of double track are supported directly to the sleepers, then to the bridge stringers by the concept of rigid links and the connector sections as defined by ABAQUS. Regarding the train bogies, each sprung mass of the wheel was considered fixed at the first second of analysis before the train is moving by assigning a gravity load on the whole model to stabilize the dynamic model. The wheel rotated by a coupling constraint established on wheel perimeter. Wheel rotation numbers and duration of the dynamic step were calculated from the simple equation of the speed, velocity, and distance, as shown in fig. 11.



| STEP TIME CALCULATION AND WHEEL ROTATION | | | | | |
|--|-------|------|---------------------------------|-------------|---------|
| wheel Dia. | 80 | cm | wheel perimeter(x) | 2.513274123 | m |
| v=L/T | 300 | kmph | no. of rotation/sec=(v*1sec/x) | 33.1873 | rad/sec |
| L=n*(2*pi*r) | 127.2 | m | Dist. at specific time | 31.2 | m |
| T | 1.526 | sec | required time at specific Dist. | 0.3744 | sec |

Fig. 11. FEM and Excel sheets screen shots of the assigned rotations in the FEM

3.4 Simulation Model of Track Defects on rail and wheel

The method of the power spectral density (PSD) function was applied as a suitable function for simulation of various defects (vertical, horizontal 4-5 mm, and cross-level 1.5 mm) [20]. In the current study the simulation of track defects was established following [5], in which the defects of various sizes and depths above the PSD limits were examined regardless of the wheel flat defect. The track defects simulated in this study are shown in figs. 12-14. They were drawn briefly with the defects' dimensions shown in Table 2.

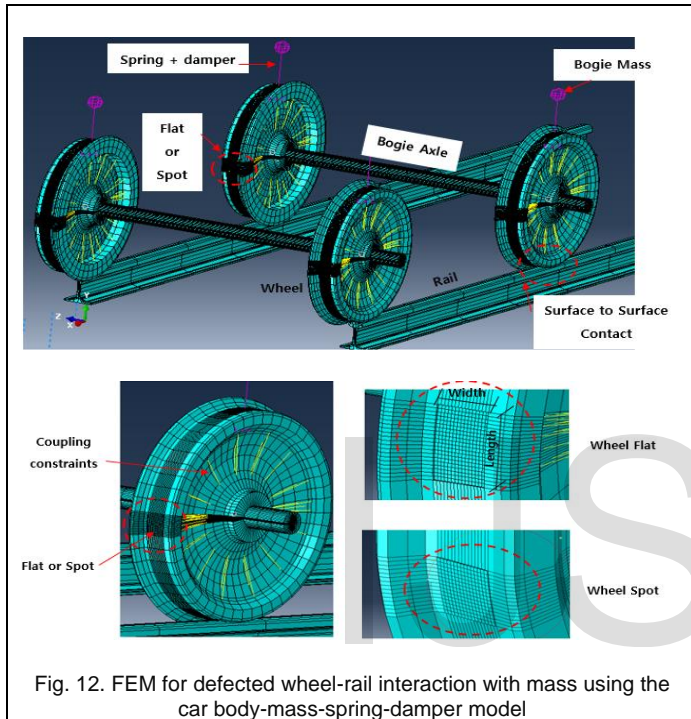


Fig. 12. FEM for defected wheel-rail interaction with mass using the car body-mass-spring-damper model

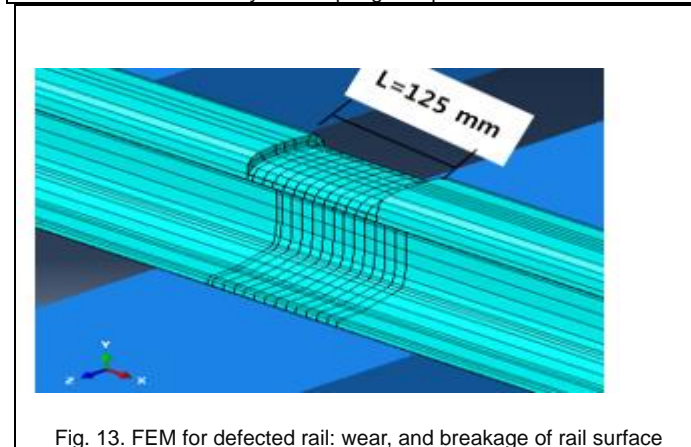


Fig. 13. FEM for defected rail: wear, and breakage of rail surface

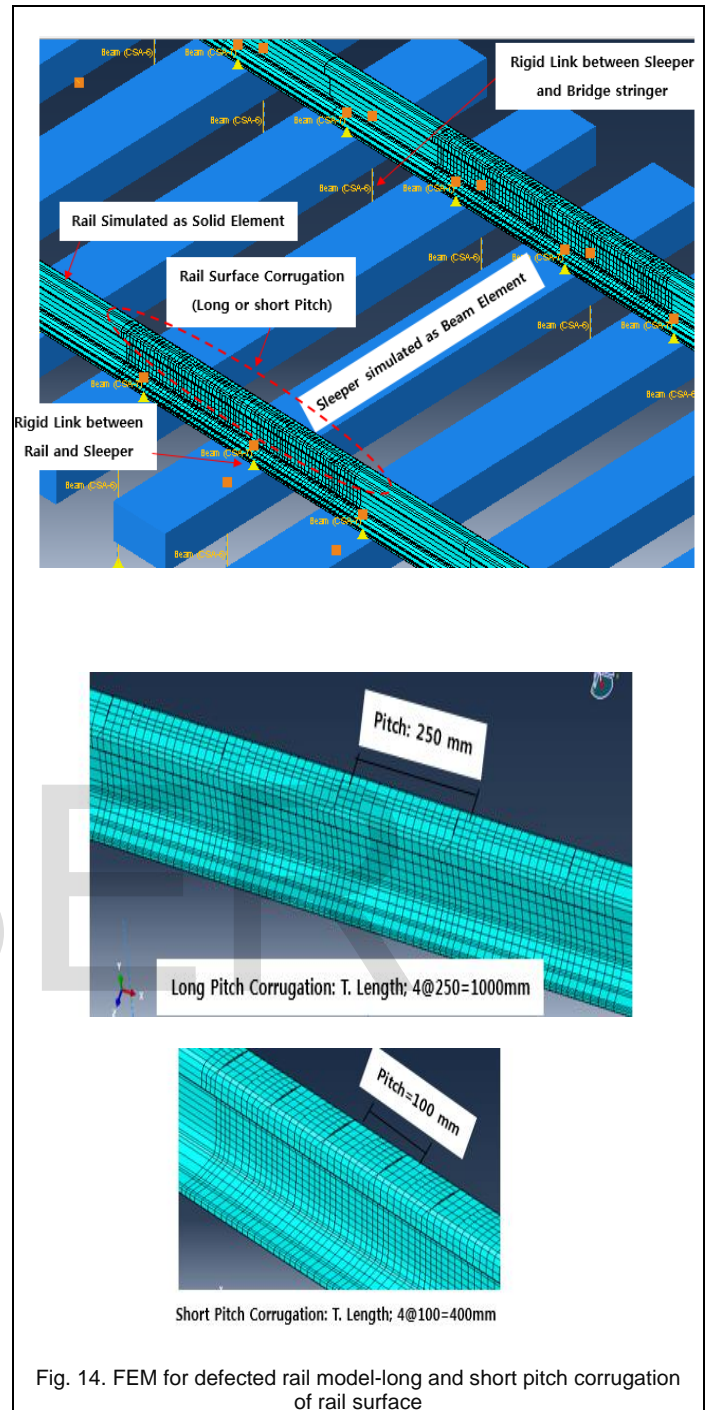
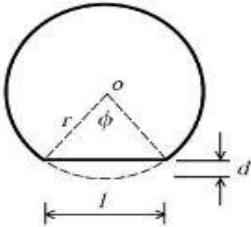
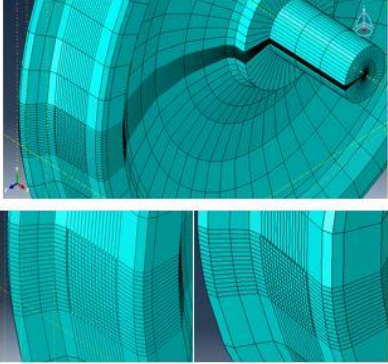
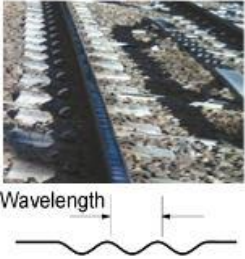
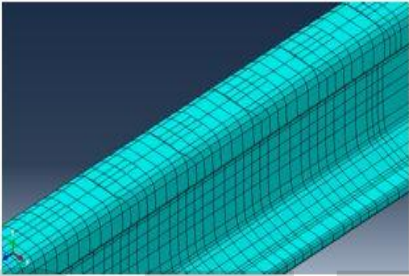

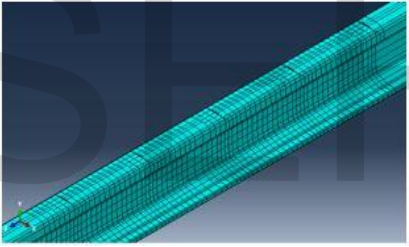
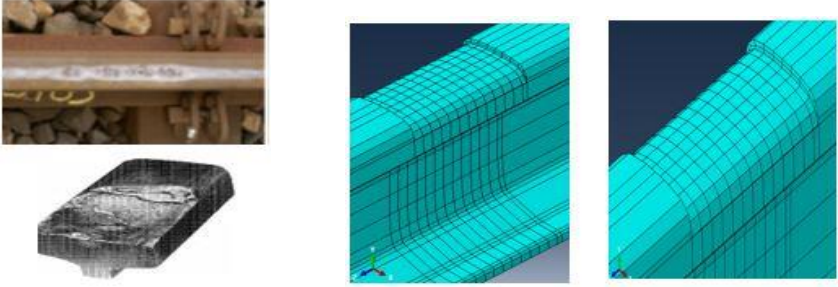
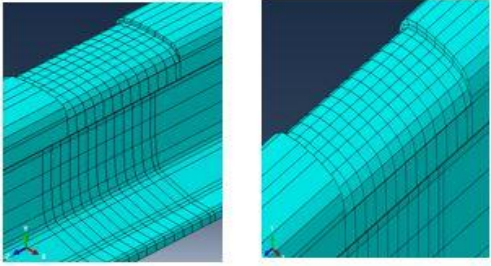


Fig. 14. FEM for defected rail model-long and short pitch corrugation of rail surface

TABLE 2
DIFFERENT CASES OF WHEEL AND RAIL DEFECTS USED IN THIS STUDY (CONT.)

| Type | Size (mm) | Shape or Schematic | Simulated Shape |
|--|-----------------|--|--|
| Wheel Flat or Spot Defect* (Length, Width, Depth) | FL. 90x60x3 |  |  |
| | FL. 80x60x2 | | |
| | FL. 60x60x1 | | |
| | Sp. 60x60x1 | | |
| Short Pitch Corrugation* (Wavelength, Depth) | S.P. 100x0.5 |  |  |
| | S.P. 100x3.0 | | |
| Long Pitch Corrugation* (Wavelength, Depth) | LP. 250x0.5 |  |  |
| | LP. 250x3.0 | | |
| Rail Breakage or Wear* (Length, Depth) | BR. 125x2.5 |  |  |

*All Rail defects are in the middle of first span of the bridge

4. VALIDATION OF THE TTB MODEL

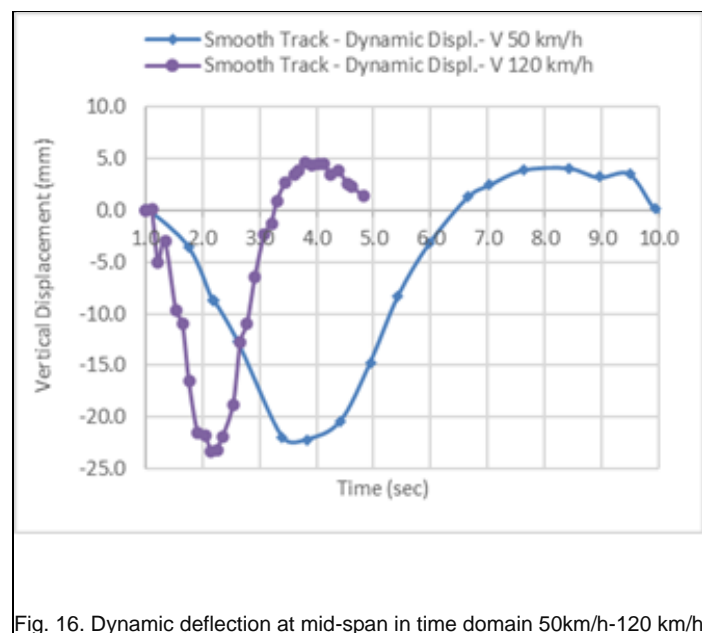
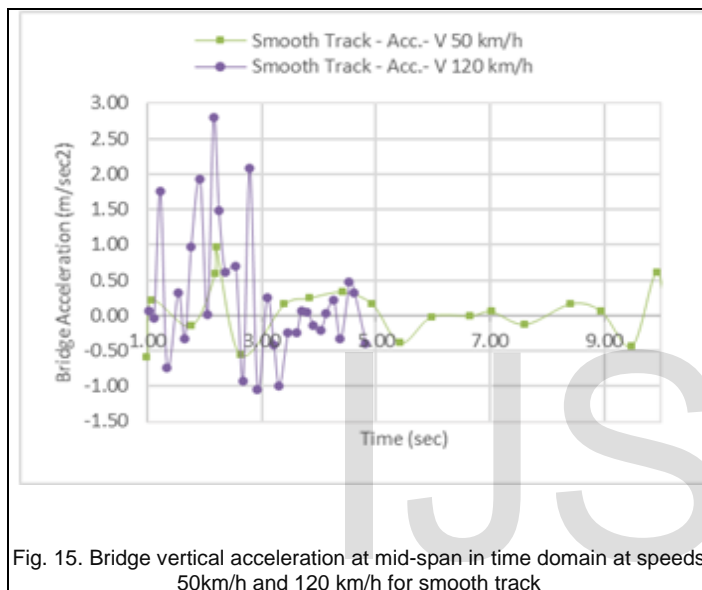
Dynamic analysis was established to determine the vertical acceleration and dynamic response of the displacement (dynamic factor). The dynamic model of TTB was simulated by considering a weld defect as a vertical dip (step-up) 7.5mm on the welded rail joint near mid-span. The results of TTB model for smooth track and the track with weld defect were compared with the driving safety requirements recommended by international codes [4, 5] as shown in Table 3, where the max

imum evaluated response was compared with the allowable values specified by code.

Figs. 15, 16 presented the time history chart of the maximum vertical acceleration at mid-span for smooth track at speeds 50km/h and 120 km/h, indicating that the maximum acceleration was within the allowable values presented by codes, ($a_{max} \leq 5 \text{ m/s}^2$).

TABLE 3
COMPARISON BETWEEN BRIDGE ACCELERATION WELD DEFECT SIMULATION RESULTS AND [4, 5] AT SPEED 120 KM/H

| Specs | a max [4, 5] | a max FEM |
|--------------------------|------------------------------|--|
| | | Smooth track: a max $\leq 2.8 \text{ m/s}^2$ |
| Driving safety of trains | a max $\leq 5 \text{ m/s}^2$ | Track with weld defect (7.5mm dip): a max $\leq 3.21 \text{ m/s}^2$ |



The ABAQUS TTB models provided in this study were used to investigate the influence of track defects on the bridge response compared with the case of smooth track (track without defects). The dynamic analysis responses have been investigated when the train passed through the bridge at a speed of 120 km/h. The bridge mid span acceleration, displacements, and strains were determined. The response of the bridge track system due to the simulated track defects was described by means of displacement and strain-based dynamic amplification factors, DAF_U and DAF_ϵ respectively, as well as bridge accelerations. DAF_U and DAF_ϵ were calculated by dividing the responses (deflection, strain) at mid-span of the bridge bottom chord or at a specific point at the stringer and cross girder associated with each defect by those responses corresponding with smooth track. It is important that the DAF_U is corresponding to “ $1+\phi$ ” which represent the effect of track irregularities in the dynamic amplification factor recommended by codes. The below graphs explain the different values of DAF_U and DAF_ϵ of FEM in comparison with the standard codes.

5.1 Effect of Track Defect on Bridge DAF_U

Fig. 17 presented the DAF_U due to different wheel and the rail defect types at train a speed of 120 km/h. It can be concluded that the dynamic amplification for defected track did not exceed 10% of the values obtained for a smooth track, however, weld defect behaved as a step up on the rail top surface causing the wheel to fly over the rail surface and generate negative effect on the displacement, that can be considered a critical case. However, the results turned out unfavourably when compared with the DAF_U recommended by codes for some specific defects’ sizes as calculated in Table 4. Since the code equations of track irregularities did not cover all types of defects that can be found on the track, further studies are required to cover this area.

FEM results for the dynamic factor due to perfected track is obtained as, $\dot{O}_{dyn}=0.054$ corresponding to, $\dot{O}_{dyn}=0.0675$ as per [4, 5] recommendation. This mean that the FEM can be in a proper agreement when compared with codes for perfected track.

5. RESULTS AND DISCUSSION

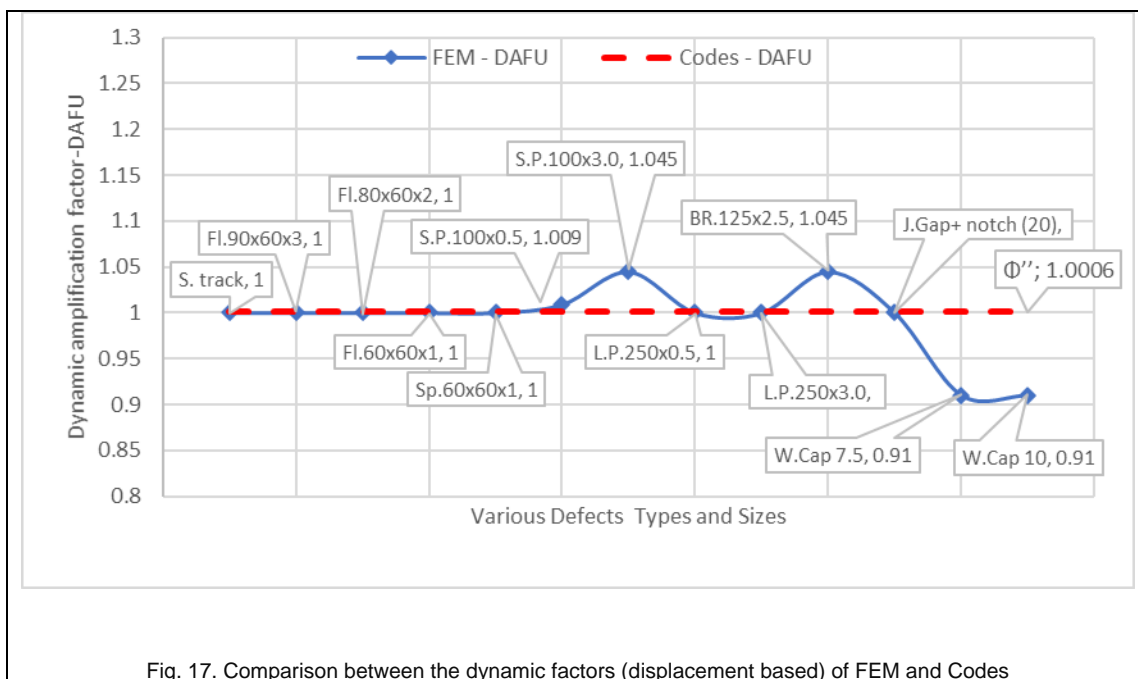


Fig. 17. Comparison between the dynamic factors (displacement based) of FEM and Codes

TABLE 42
DYNAMIC AMPLIFICATION FACTOR CALCULATION ACCORDING TO CODES ([1+ ϕ + ϕ'])

| Calculation according to EN 1991-2(2003) | [4, 5] | FEM |
|---|--|---|
| $\phi' = \frac{K}{1 + 0.001K}$ for $K < 0.76$ $\phi' = 1.325$ for $K \geq 0.76$ $K = \frac{V}{\dots}$ | (EN.-C3) (EN.-C4) (EN.-C5) | $\phi_{dyn} = 0.054$ |
| $\phi'' = \frac{\alpha}{56} [56e^{-\frac{100}{10}} + 50(\frac{100 \cdot \alpha \alpha}{\dots} - 1)e^{-\frac{100}{10}}] \geq 0$ (EN.-C6) | $V = 120 \text{ km/h}$ $K = 0.0756$ $n_o = 3.455$ $\phi = 0.0675$ | |
| $\alpha = \frac{v}{22}$ for $v \leq 22 \text{ m/s}$ $\alpha = 1$ for $v > 22 \text{ m/s}$ | (EN.-C7) (EN.-C7) | |
| where, ϕ' dyn represent the effect of track in perfect geometrical condition, and ϕ'' represent the effect of track irregularities. | | |
| $\phi' = \frac{K}{1 + 0.001K}$ for $K < 0.76$ $\phi' = 1.325$ for $K \geq 0.76$ $K = \frac{V}{\dots}$ | (EN.-C3) (EN.-C4) (EN.-C5) | $\phi_{dyn} = 0.009$ for the case of short pitch corrugation with 0.5mm depth $\phi''_{dyn} = 0.054$, for the case of short pitch corrugation with 3mm depth and case of rail breakage |
| | $V = 33.33 \text{ m/s}$ $n_o = 3.455$ $\alpha = 1$ $\phi'' = 0.00006$ | |

5.2 Effect of Track Defect on The Strain of Bridge Elements

5.2.1 Strain of Stringers and Cross Girders

Regarding strain of stringer and cross girder, the strain-based dynamic amplification factor DAF ϵ is plotted in Fig. 18 for different wheel and the rail defect types.

- The response for all defects inherent with the dynamic amplification of the cross girder did not exceed

10%.

- The strain of stringers was increased by 20%, that can be attributed to the direct fixation of rails to stringers.
- Pitch corrugation is the most effective defect on the stringer strain.
- Wheel flat with 3mm depth is the most critical depth as the strain-based dynamic factor reaches 15%, whereas the values dropped to approximately 10% with 2mm depth.

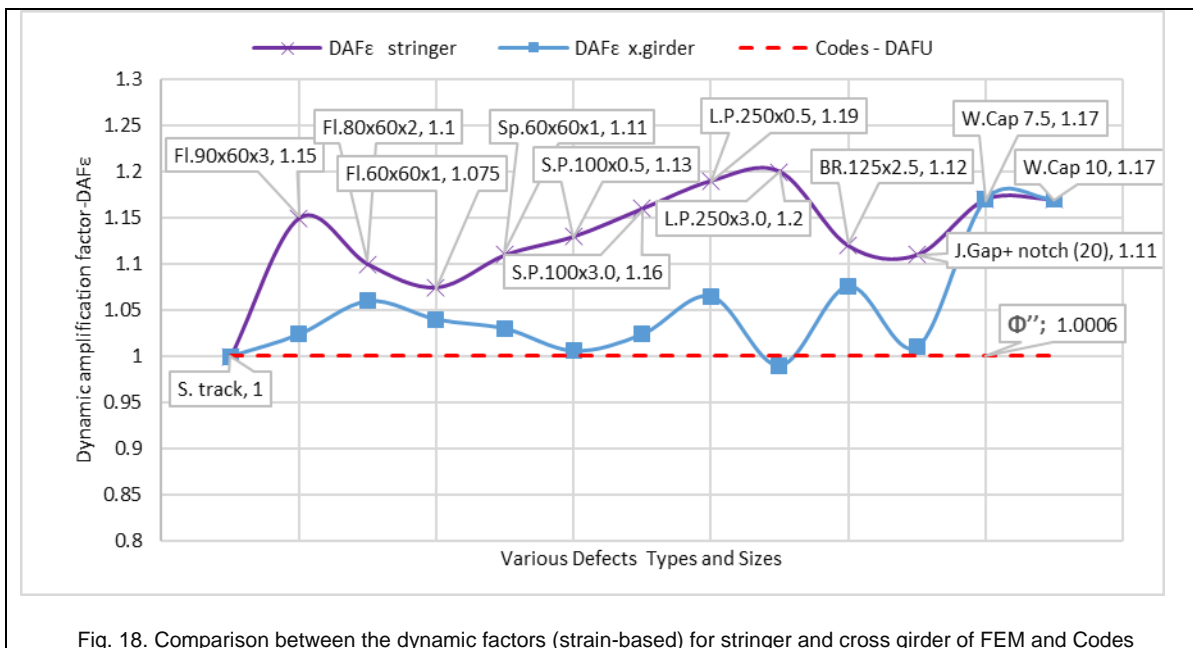


Fig. 18. Comparison between the dynamic factors (strain-based) for stringer and cross girder of FEM and Codes

5.2.2 Strain of Main Truss Bottom Chord

regarding the strain of Main truss bottom chord at mid span, the strain-based dynamic amplification factor DAF_{ϵ} is plotted in fig19 for the different types of wheel and rail defect.

- The bottom chords of the main truss at the mid-span are greatly affected by the pitch corrugation of 3mm depth, weld defects, and wheel flat defects that were increased by 13%, 10%, respectively.
- Pitch corrugation is the most crucial defect on the main truss elements, as the dynamic factor of strain-

based reaches 13%.

- Wheel flat defects and rail weld defects have also a critical effect on the strain of main truss chords as the dynamic factor of strain-based reaches 10%.
- The effect of track defects on the bridge element strains are neglected by the international codes. Only the dynamic amplification factor on the displacement based is considered.

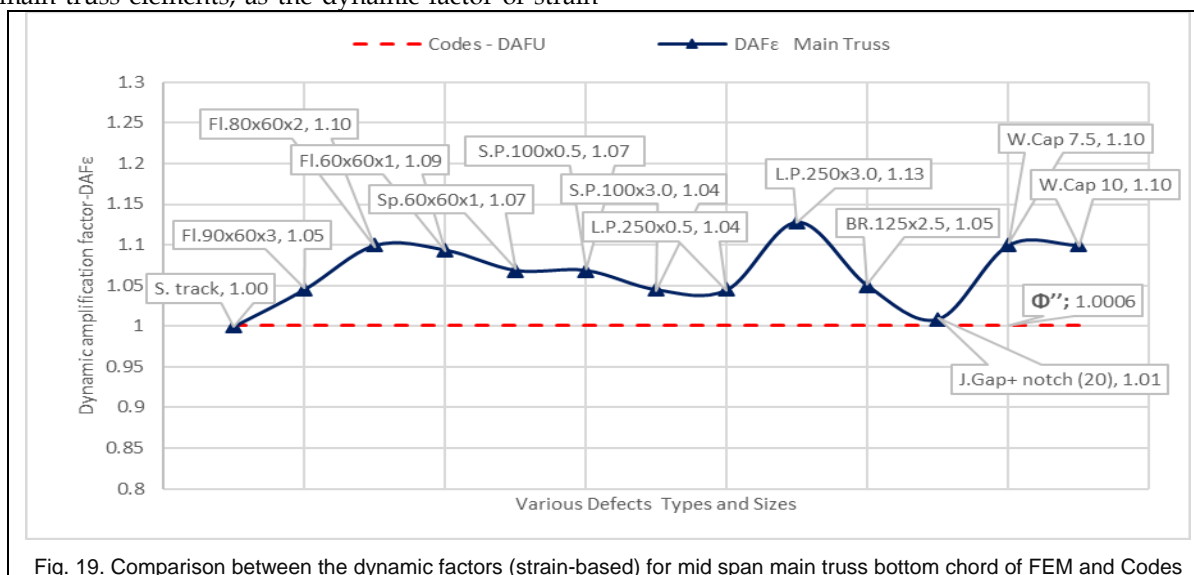


Fig. 19. Comparison between the dynamic factors (strain-based) for mid span main truss bottom chord of FEM and Codes

5.3 Effect of Track Defect on Bridge Acceleration

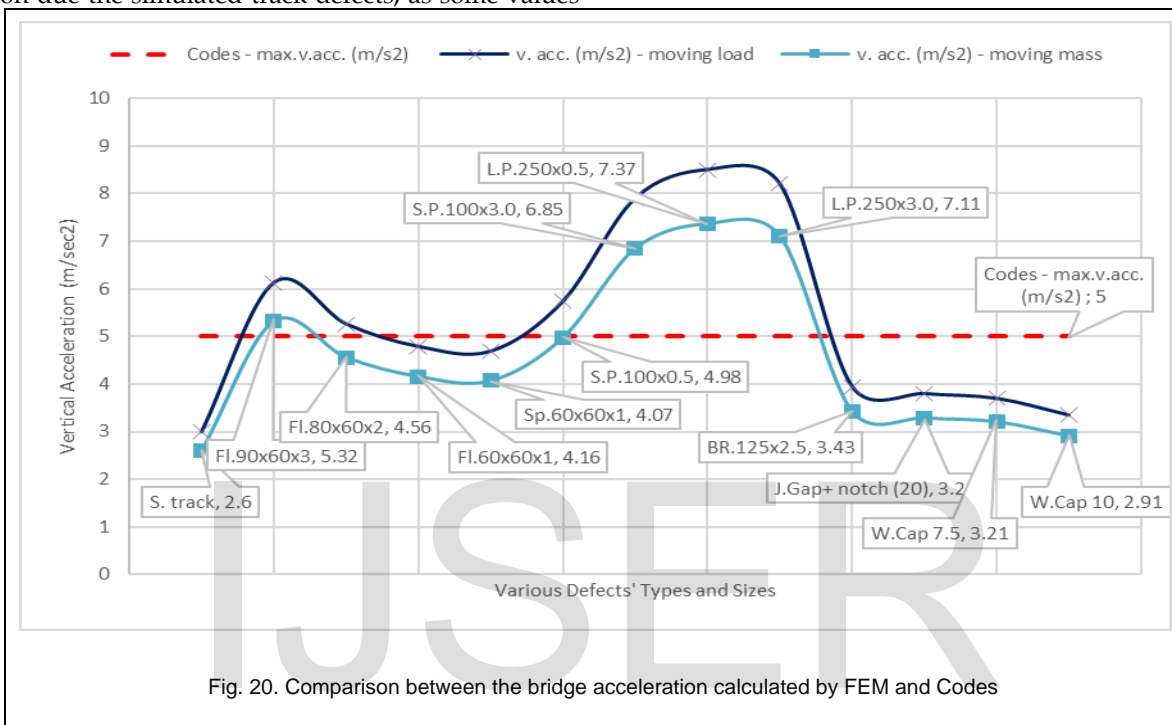
Fig. 20 show the bridge vertical acceleration due to different

types of simulated track defects, assigning train load modelled either as a series of moving loads or sprung masses.

- The inclusion of the inertial effect of the moving trains by the sprung mass model resulted in slight reduction of the bridge's peak response since the sprung mass behaved in some sense that resembled tuned mass to the bridge. The bridge acceleration decreased by about 13% when moving of sprung mass was used.
- A significant effect was noticed on the bridge acceleration due the simulated track defects, as some values

exceeded the allowable limit proposed by the international codes ($a_{max} \leq 5 \text{ m/s}^2$). Pitch corrugation is the most critical defect on the bridge acceleration, as the values exceeded the allowable limits recommended by [4, 5].

- Depth of 3mm for the wheel flat is critical as the bridge acceleration exceeds the allowable limits advised by codes.



5.4 Influence of Rail Corrugation Defects on the Bridge Response

A short and long pitch rail corrugation 100mm and 250mm, respectively were extensively simulated in depths within 0.5 to 3mm and applied on the TTB model. The results indicated that rail corrugation had a great influence on the vertical acceleration of the bridge, as it increased the maximum values recommended by standards and codes. In addition, long pitch corrugation has greater effect than the shorter one on the bridge acceleration.

A negative acceleration was recorded just before a shock pulse

at 3mm depth caused by the so called 'wheel fly' effect that usually occurs when the wheel treads leave the railhead due to gaps in either short or long-pitch corrugations on the rail, subsequently, the wheel strikes the railhead with the axle sprung mass weight. Meanwhile, the strain of stringer has been affected drastically where DAF_e was increased from 13% to 20% due to different depths and pitches of corrugation. On the contrary, the cross-girder strain was increased within 10% since, the track was fixed directly to the stringer. The vertical acceleration and displacement at mid-span for short and long pitch corrugation were plotted in time domain as shown in figs. 21, 22.

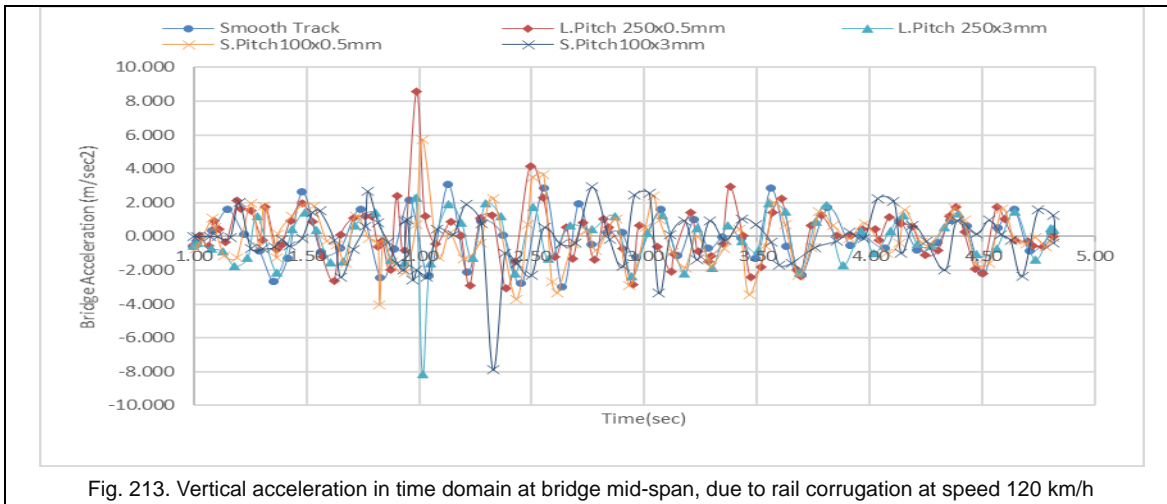


Fig. 213. Vertical acceleration in time domain at bridge mid-span, due to rail corrugation at speed 120 km/h

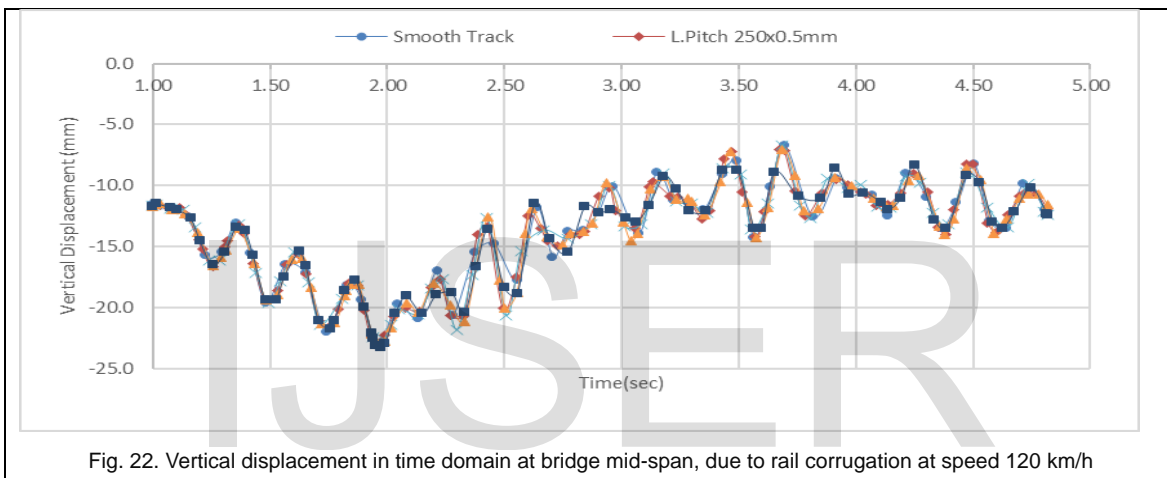


Fig. 22. Vertical displacement in time domain at bridge mid-span, due to rail corrugation at speed 120 km/h

5.5 Influence of Wheel Flat or Spot Defects on the Bridge Response

In this study, a fresh and worn out flat of 60, 80, and 90mm long in 1, 2, and 3mm depth, respectively were simulated on the TTB model. The results indicated that the wheel flat has a great influence on the vertical acceleration of the bridge. The case of wheel flat 90x3mm exceeded, the maximum values

recommended by [4, 5], and the stringer strain was increased by 15% when compared with perfected track. Results also showed that, the wheel spot and flat could have the same effect on the bridge acceleration and strains. The vertical acceleration and displacement at mid-span for wheel flat defects were plotted in time domain as shown in Figs. 23, 24.

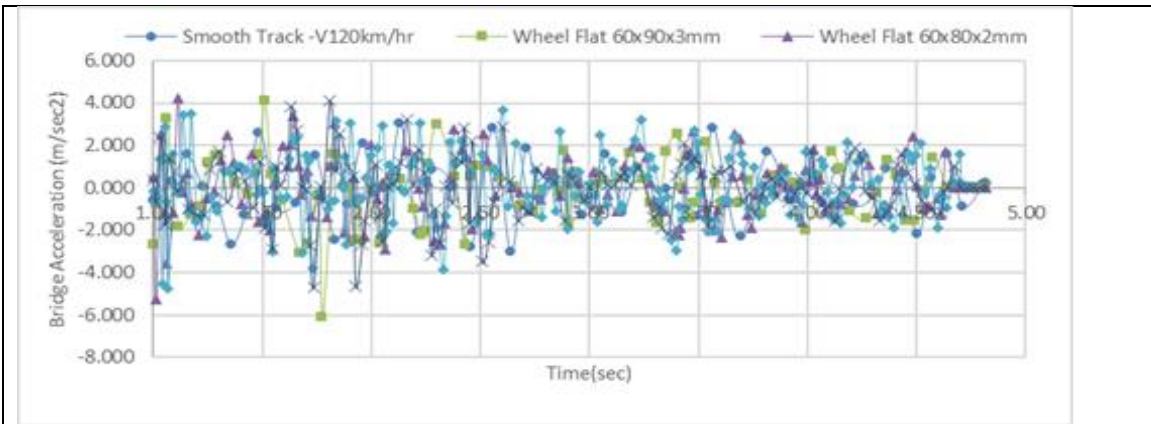


Fig. 4. Vertical acceleration in time domain at bridge mid-span due to wheel flat defects at speed 120 km/h

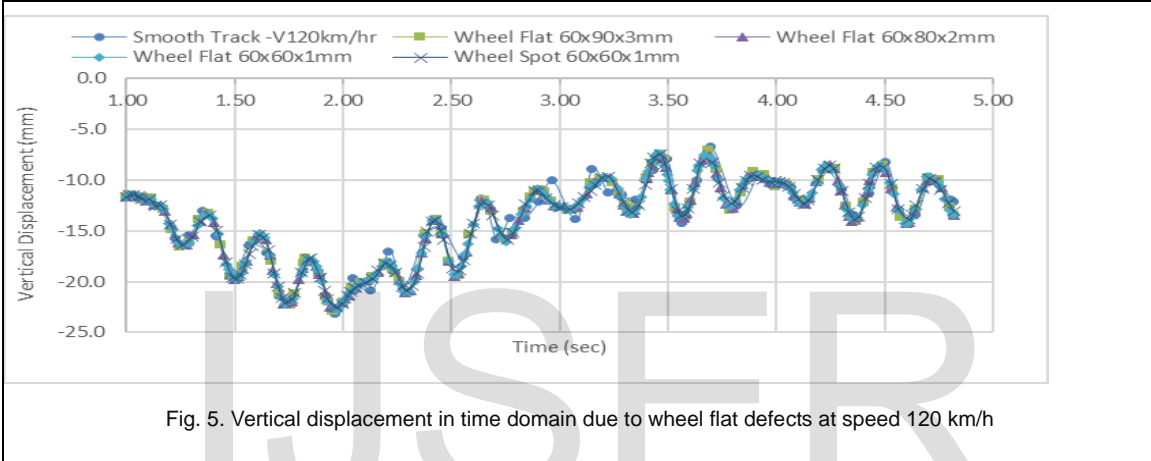


Fig. 5. Vertical displacement in time domain due to wheel flat defects at speed 120 km/h

5.6 Influence of Rail Breakage Defects on the Bridge Response

In this study, a sample of step-down defects in 125mm long and 2.5mm depth were simulated on the TTB model. The results show that, the vertical acceleration of the bridge was increased by 32% when compared with perfected track and can exceed the maximum values recommended by standards. Results also show that the strain of stringer can be affected drastically, the DAF_ε was increased from 12% because of step down 2.5 mm. The vertical acceleration and displacement at mid-span for step down defects were plotted in time domain as shown in Figs. 25, 26.

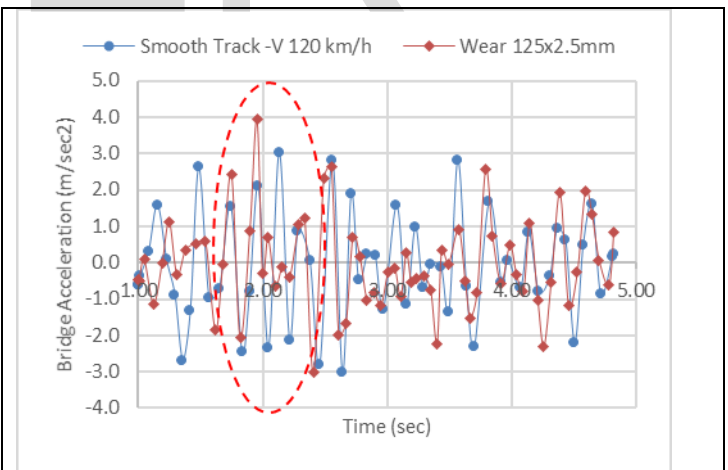


Fig. 25. Vertical acceleration in time domain due to breakage or step-down defects

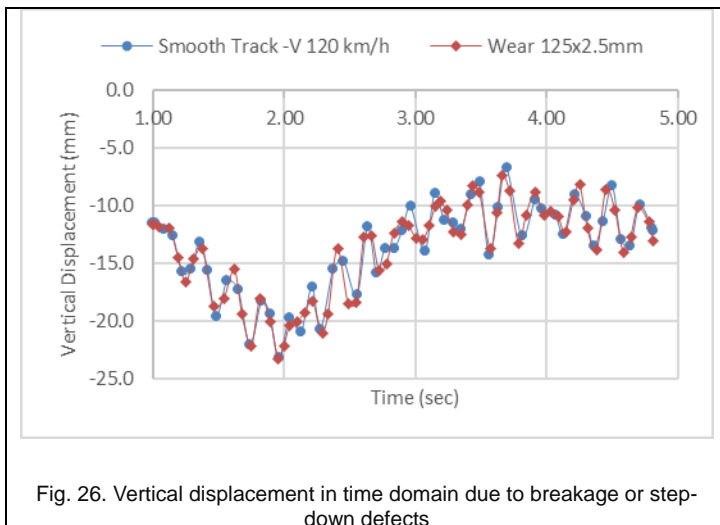


Fig. 26. Vertical displacement in time domain due to breakage or step-down defects

6. CONCLUSIONS

Based on the numerical dynamic analysis of TTB models prepared by the authors and verified partially with international ode equations [4, 5], we can generally conclude that:

- The response associated with all defects at a speed of 120 km/h inherent with the dynamic amplification did not exceed 10% of the values obtained for a smooth track which is unfavourably compared to the DAF_U recommended by codes for some specific sizes of defects. Meaning that, code equation of track irregularities does not cover all types of defects that can be found on the track, consequently further studies are required for full coverage of tracks' defects.
- The effect of strain response is neglected by codes.
- The response for all defects inherent with the dynamic amplification of the cross girder did not exceed 10%.
- The strain of stringers was increased by 20%. This can be attributed to the direct fixation of rails to stringers, most likely due to direct fixation of track with stringers.
- A significant effect on the bridge acceleration was noticed due the simulated track defects. Furthermore, some values exceeded the allowable limit proposed by the international codes, ($a_{max} \leq 5m/s^2$).
- Pitch corrugation is the most critical defects on the bridge acceleration whose values exceed the allowable limits recommended by codes. Also, it has a critical effect on the strain of the stringer.
- Wheel flat with depth of 3mm is as the bridge acceleration exceed the allowable limits advised by codes. It, moreover, has a critical effect on the strain of the bridge's element specifically on the stringer, where the dynamic factor of train based was increased by 15% comparing with perfected track.
- Regarding assigning the load either as a moving load or a sprung mass, the effect of the assigned train load modelled either as a series of moving loads or sprung

masses on the bridge have variable responses.

- The bridge acceleration has decreased by 13% when moving of sprung mass was used. Also, a minor effect was found on the displacement and strain. where the sprung mass behaviour resembled the tuned mass on the bridge
- At speed 120 km/h the vertical acceleration of the studied bridge was increased from $2.6m/s^2$ to $7.43m/s^2$ due to the assigned track defect. Furthermore, the values exceeded the allowable limits recommended by code.
- The presence of track defects specifically when the tracks are fixed directly to the bridge requisite precise monitoring and close follow-up during track maintenance since the quality of track maintenance has a direct impact on the bridge response and the safety values of accelerations recommended by standard codes, in addition to their influence in increasing the strains and stresses of the bridge's elements.

REFERENCES

- [1] J. F., Unsworth, (2010), "Design of Modern Steel Railway Bridges", CRC Press Taylor and Francis Group; Reference to a Chapter: Chapter 3, P. 77-80.
- [2] W., Zhai and C.B., Cai. (2002), "Train-Track-Bridge Dynamic Interactions: Simulation and Applications", J. Vehicle System Dynamics; 37:sup1, 653-665, <https://doi.org/10.1080/00423114.2002.11666270>.
- [3] International Union of Railways. UIC Code 776-1R., (2006), "Loads to be Considered in Railway Bridge Design". Paris.
- [4] EN 1991-2 (2003), "Eurocode 1, Actions on Structures, Part 2, "Traffic Loads on Bridges", Annex C: Dynamic factors for real trains.
- [5] International Union of Railways. UIC Code 712-R. (Translation 4th Edition, January 2002), "Rail Defects". Paris.
- [6] L.R.T., Melo, D., Ribeiro, R., Calçada & T.N., Bittencourt, (2019), "Validation of a vertical train-track-bridge dynamic interaction model based on limited experimental data", Structure, and Infrastructure Engineering, DOI: 10.1080/15732479. 2019.1605394
- [7] F.T.K. Au, J.J. Wang, Y.K. Cheung. (2002), Impact Study of Cable-Stayed Railway Bridges with Random Rail Irregularities. J. EngStruct. 24 (2002) 529-541, PII: S0141-0296(01)00119-5
- [8] J., Malveiroa, C., Sousab, D., Ribeiroc, R., Calçadad, (2018), "Impact of Track Irregularities and Damping on the Fatigue Damage of A Railway Bridge Deck Slab", J. Structure and Infrastructure Engineering; <https://doi.org/10.1080/15732479.2017.1418010>
- [9] D., Canteroa, T., Arvidsson, E., Obrienb, R., Karoumia, (2016), "Train-Track-Bridge Modelling and Review of Parameters", J. Structure and Infrastructure Engineering, 12:9, 1051-1064, <https://doi.org/10.1080/15732479.2015.1076854>.
- [10] Michal Majka A, Michael Hartnett. (2009), "Dynamic Response of Bridges to Moving Trains: A Study on Effects of Random Track Irregularities and Bridge Skewness", J. compstruc. 87 1233-1252, doi: 10.1016/j.compstruc.2008.12.004.
- [11] M., Klasztorny, M., Podworna, (2014), "Influence if Random Track Irregularities on Dynamic Response of Bridge - Track Structure - High-Speed Train Systems", A. Cunha, E. Caetano, P. Ribeiro, G. Müller (eds.). In: Porto, Portugal, 30 June - 2 July, Proceedings of the

9th International Conference on Structural Dynamics, EUROODYN 2014; ISSN: 2311-9020; ISBN: 978-972-752-165-4.

- [12] G., Kouroussis, David P., "Connolly B, Georgios Alexandrou A, Konstantinos Vogiatzis", (2015), The Effect of Railway Local Irregularities on Ground Vibration. *J. Transportation Research Part D* 39 (2015) 17-30, <http://dx.doi.org/10.1016/j.trd.2015.06.001>
- [13] U. Zerbst, R. Lundén, K.-O. Edel, R.A. Smith. (2009), "Introduction to the Damage Tolerance Behaviour of Railway Rails-a Review", *J. Engng Fract Mech* 76 2563-2601.
- [14] A. M., Remennikov, S., Kaewunruen, (2008), "A Review of Loading Conditions for Railway Track Structures Due To Train and Track Vertical Interaction", *J. Struct. Control Health Monit.*; 15:207-234, <https://doi.org/10.1002/stc.227>.
- [15] Z., Li , X., Zhao, R., Dollevoet, M., Molodova. (2008), "Differential wear and plastic deformation as causes of squat at track local stiffness change combined with other track short defects", *International Journal of Vehicle Mechanics and Mobility*, 46:S1, 237-246, <http://dx.doi.org/10.1080/00423110801935855>.
- [16] W., Zhai, Z., Han, Z., Chen, L., Ling & S., Zhu (2019), "Train-track-bridge dynamic interaction: a state-of-the-art review, *Vehicle System Dynamics*", 57:7, 984-1027, DOI: 10.1080/00423114.2019.1605085
- [17] M., Saber, (2020)," Structural Behaviour of Railway Steel Bridges Due to Rail Defects.", M.Sc. Thesis, Faculty of Engineering at Shoubra, Benha University, Egypt.
- [18] H., H., Eltobgy, A. A. M., Khalil, E., Darwish, M., Saber, "Effect of Rail Welding Defects on the Railway Steel Bridges Response", *International Journal of Scientific & Engineering Research* Volume 11, Issue 1, January-2020, pp 578-585.
- [19] ABAQUS Version CAE (2017), Dassault Systèmes Simulia Corp., Providence, RI, USA.
- [20] Y. B. Yang, J. D. Yau, and Y. S. Wu. (2004), "Vehicle-Bridge Interaction Dynamics with Applications to High-Speed Railways", *World Scientific Publishing Co.* chapters: Ch.1, p. 20-23; Ch.4, p. 108-110; Ch.6, p.184; Ch.7, p.220-221; Ch.10, p. 354-361.